8222 *Inorg. Chem.* **2010**, *49*, 8222–8229
DOI: 10.1021/ic101167f

Inorganic Chemistry
Article

Nickel(II)-Dipeptidoamine-Based Tetrameric Complex: Structural Study in Solution and in Solid State

Katalin Selmeczi,*,† Patrick Gizzi,† Delphine Champmartin,† Patrice Rubini,† Emmanuel Aubert,‡ Slimane Dahaoui,‡ and Bernard Henry*,†

†*Laboratoire SRSMC (UMR 7565 CNRS - Université Henri Poincaré Nancy 1), Nancy Université, BP 70239, F-54506 Vandoeuvre-lès-Nancy Cedex, France, and* ‡*Laboratoire CRM² (UMR 7036 CNRS - Université Henri Poincaré Nancy 1), Nancy Université, BP 70239, F-54506 Vandoeuvre-lès-Nancy Cedex, France*

Received January 19, 2010

The coordination structure of $M_4L_4H_{-8}$ macromolecules (M = Ni(II), Cu(II), Pd(II)) containing small peptidic ligands (L = Xaa-His or Xaa-His-Yaa) has been predicted primarily on the basis of spectroscopic and potentiometric data in the literature. In this work, the neutral tetranuclear nickel(II) complex **1** formed with four double-deprotonated ligands (L = α-methyl-alanyl-histamine) was prepared, and its crystal structure was determined ($C_{36}H_{56}N_{16}Ni_4O_4 \cdot 4.5CH_3OH \cdot 1.5H_2O$: a = 11.2645(4) Å, b = 23.5003(8) Å, c = 20.9007(7) Å, β = 102.321(1)°, monoclinic, $P2_1/c$, Z = 4). In complex **1**, the metal ions have a square planar geometry with 4N donor set consisting of the N-terminal amino nitrogen, the deprotonated amide nitrogen, the imidazole N^3 atom, and the deprotonated imidazole N^1 atom of the adjacent ligand. The latter nitrogen atom provides the connection of the four $NiLH_{-2}$ units forming a C_1 symmetrical saddle-like shape. The complexation of L with Ni(II) ion has been studied by a potentiometric method combined with UV−visible spectrophotometric titration. At pH 8.0, the predominant species is $M_4L_4H_{-8}$ with $pK^4_{oligomerization}$ = 5.73. The tetranuclear structure of complex **1** was also studied in solution by ^1H and ^{13}C NMR spectroscopy suggesting a structure of symmetry S_4. DFT calculations on optimized structure in symmetry C_1 and S_4 have been performed to explain the observed differences in solution and in solid state. The nuclearity was also confirmed in solution by ESI-HRMS analysis.

Introduction

Metalloenzymes usually contain metal ions bound to a specific amino acid residue of peptide backbone, for example, the imidazole group of histidine. Imidazole can bind metal in different ways: more often as monodentate ligand via N^3 nitrogen (IUPAC convention, pyridine-like) or, in some cases, as bidentate bridging ligand between two metal centers via N^3 and deprotonated N^1 (pyrrole-like) nitrogens. The first binding mode has already been extensively studied with histidine or histamine containing di-, tri-, or oligopeptide in the presence of Cu^{II}, Ni^{II}, Co^{II}, and Zn^{II} ions.[1] Fewer efforts have been paid to analyze the structure of the pyrrole-like coordination mode in peptidic environment. In free ligand, the imidazole-N^1−H is a very weak acid (pK > 14) and does not participate in metal binding. However, metal ion coordination to N^3 induces the N^1−H deprotonation across the imidazole ring. Xaa-Yaa-His tripeptides form 4N-type (N_{amine}, $2N_{amide}$, N^3_{im}) monomeric species in physiological pH-range, and further deprotonation of N^1 nitrogen was observed at pH > 10 without metal coordination to the latter.[2] The insertion of histidine or histamine in position 2 of the peptide chain (Xaa-His or Xaa-His-Yaa) results in the major 3N-type complex (N_{amine}, N_{amide}, N^3_{im}). The most characteristic feature of these short peptides is the formation of stable tetrameric $M_4L_4H_{-8}$ complex with square-planar metal ion bridged by N^1-imidazole nitrogens at alkaline pH. Such a cyclic tetramer has been proposed for copper(II), nickel(II), and palladium(II) containing di- or tripeptide[3−8] primarily on the basis of potentiometric and spectroscopic data in solution (UV−vis, NMR, EPR). Until now, the only crystal structure has been obtained for gold(III) glycyl-L-histidine,

*To whom correspondence should be addressed. E-mail: katalin.selmeczi@srsmc.uhp-nancy.fr (K.S.), bernard.henry@srsmc.uhp-nancy.fr (B.H.).

(1) Kozlowski, H.; Kowalik-Jankowska, T.; Jezowska-Bojczuk, M. *Coord. Chem. Rev.* **2005**, *249*, 2323. Sóvágó, I.; Ösz, K. *Dalton Trans.* **2006**, 3841.
(2) Gajda, T.; Henry, B.; Aubry, A.; Delpuech, J.-J. *Inorg. Chem.* **1996**, *35*, 586. Gizzi, P.; Henry, B.; Rubini, P.; Giroux, S.; Wenger, E. *J. Inorg. Biochem.* **2005**, *99*, 1182.
(3) Bruni, S.; Cariati, F.; Daniele, P. G.; Prenesti, E. *Spectrochim. Acta, Part A* **2000**, *56*, 815. Gajda, T.; Henry, B.; Delpuech, J.-J. *J. Chem. Soc., Dalton Trans.* **1992**, 2313.
(4) Daniele, P. G.; Zerbinati, O.; Zelano, V.; Ostacoli, G. *J. Chem. Soc., Dalton Trans.* **1991**, 2711. Sóvágó, I.; Farkas, E.; Gergely, A. *J. Chem. Soc., Dalton Trans.* **1982**, 2159. Árkosi, Z.; Paksi, Z.; Korecz, L.; Gajda, T.; Henry, B.; Rockenbauer, A. *J. Inorg. Biochem.* **2004**, *98*, 1995.
(5) Gajda, T.; Henry, B.; Delpuech, J.-J. *J. Chem. Soc., Dalton Trans.* **1993**, 1301.
(6) Gajda, T.; Henry, B.; Delpuech, J.-J. *Inorg. Chem.* **1995**, *34*, 2455.
(7) Mlynarz, P.; Kowalik-Jankowska, T.; Stasiak, M.; Leplawy, M. T.; Kozlowski, H. *J. Chem. Soc., Dalton Trans.* **1999**, 3673.
(8) Morris, P. J.; Martin, R. B. *J. Inorg. Nucl. Chem.* **1971**, *33*, 2913.

 Published on Web 08/19/2010

where the strong polarizing power of Au^{III} (5d metal) favors the imidazole N^1-H deprotonation at relatively low pH (6−7) and thus induces the cyclic tetramer formation.[9]

It should be mentioned that the pH-induced monomer−oligomer interconversion of imidazole-containing coordination compounds with nonpeptidic ligands has been studied, and the structure of oligonuclear (tetra- or hexanuclear) species has already been determined. The factors controlling the characteristics (nuclearity, shape) of the self-assembly process have also been examined.[10,11]

In this work, we report the first structural characterization of cyclic tetramer formed by a 3d transition metal and an original pseudodipeptidic ligand, namely, the tetranuclear nickel(II) complex of α-methyl-alanyl-histamine (αMeAla-Ha).

Experimental Section

General Remarks. All chemicals were of reagent grade and used without purification. ^1H and ^{13}C NMR spectra were recorded on Bruker-DRX400 operating at 400.13 MHz for ^1H and 100.61 MHz for ^{13}C. The chemical shifts δ were measured with respect to MeOH signal (3.31 ppm for ^1H and 49.15 ppm for ^{13}C NMR) or to dioxane signal ($\delta_{dioxane}$ = 3.70 for ^1H and 67.40 ppm for ^{13}C NMR) as external reference in capillary for aqueous (H_2O) solution. The X-ray structure numbering was used for identification of H and C atoms. ESI-MS measurements were performed on Waters Platform at low resolution and on Bruker MicroTOFQ at high resolution. UV−vis spectra were recorded on a Perkin-Elmer Lambda1050 UV−vis−NIR spectrophotometer using a cell with 1 cm optical path length at T = 298 K. Elemental analysis was recorded with Thermofinnigan FlashEA 1112 elemental analyzer. Atomic absorption measurements were made on FS220 Varian atomic absorption spectrometer.

Caution! *Perchlorate salts of metal complexes with organic ligands are potentially explosive. Only small amounts of material should be prepared, and these should be handled with great care!*

α-Methyl-alanyl-histamine Dihydrochloride Salt, α-MeAla-HA·2HCl. The ligand was prepared from *N*-(*tert*-butoxycarbonyl)-α-methyl-alanine and histamine·2HCl according to a procedure described earlier.[12] The purity of this product was checked by NMR spectroscopy, elemental analysis, and acid−base titrations. Mp 244 °C. ^1H NMR (MeOH-d_4): δ 7.57 (s, 1H, (C9)H), 6.85 (s, 1H, (C8)H), 3.43 (t, ^3J = 7.04 Hz, 2H, $(C5)H_2$), 2.78 (t, ^3J = 7.04 Hz, 2H, $(C6)H_2$), 1.27 (s, 6H, $(C3)H_3$ and $(C2)H_3$). ^{13}C NMR (MeOH-d_4): δ 180.46 (C4), 136.46 (C9), 136.16 (C7), 118.25 (C8), 55.70 (C1), 40.63 (C5), 28.58 (C6), 27.88 (C3, C2). ESI-MS^+ (H_2O) m/z calculated for $[M + H]^+$ 197.14, found 197.10. Anal. Calcd. for $C_9H_{16}N_4O·2HCl$: C, 40.16; H, 6.74; N, 20.81. Found: C, 39.96; H, 6.93; N, 20.45.

Preparation of [Ni(αMeAla-Ha)]$_4$ (1). α-MeAla-HA·2HCl (5.4 mg, 0.02 mmol) dissolved in 500 μL of water was added to aqueous solution (500 μL) of $Ni(ClO_4)_2·6H_2O$ (7.3 mg, 0.02 mmol). The mixture was stirred at room temperature, 0.1 M NaOH solution was added dropwise, and the pH was measured simultaneously. Around pH 7 yellow precipitate formed slowly, and the precipitation was completed by further addition of NaOH solution until pH 10. The solid was filtered, washed with water, and dried. The product was recrystallized from MeOH. ^1H NMR (MeOH-d_4): δ 6.81 (s, 1H, (C8)H), 5.39 (s, 1H, (C9)H), 3.09 (m, 1H, $(C5)H_2$), 2.58 and 2.61 (m, 2H, $(C6)H_2$), 2.22 (m, 1H, $(C5)H_2$), 1.41 and 1.27 (s, 2 × 3H, $(C3)H_3$ and $(C2)H_3$). ^{13}C NMR (MeOH-d_4): δ 184.97 (C4), 144.40 (C9), 138.29 (C7), 122.75 (C8), 59.54 (C1), 41.35 (C5), 27.76 (C6), 27.79 and 27.31 (C3, C2). ESI-$HRMS^+$ (MeOH) m/z calculated for $C_{36}H_{56}N_{16}Ni_4O_4$ $[M+Na]^+$ 1033.2066, found 1033.2057 (0.9 mDa). UV−vis (H_2O): λ_{max} (ε) 443 nm (520 $L.mol^{-1}·cm^{-1}$).

pH-Metric Measurement. The ligand protonation and metal coordination equilibria in the pH range 3−11 were investigated by potentiometric titrations in aqueous solution (I = 0.1 M $NaClO_4$, and T = 298.0 ± 0.1 K) under argon atmosphere. The pH measurements were made with an automatic titration set including a PC controlled Metrohm Titrando 809 autoburet and an Orion Ross Semimicro combined pH glass electrode. The latter was calibrated throughout the pH range in aqueous solution (mixture of strong acid $HClO_4$ and weak acid TRIS, pK_a = 8.06) via the modified Nernst equation (eq 1).[13]

$$E = E_0 + \frac{2.303RT}{F}\log[H^+] + J_H[H^+] + \frac{J_{OH}K_w}{[H^+]} \quad (1)$$

where J_H and J_{OH} are fitting parameters in acidic and alkaline, respectively, media for the correction of experimental errors, mainly due to the liquid junction and to the alkaline and acidic errors of the glass electrode. $K_w = 10^{-13.75}$ is the autoprotolysis constant of water.[14] The parameters were calculated by nonlinear least-squares method.

The formation constants (β_{pqr}, eq 3) for the generalized reaction 2 were evaluated from the pH-metric titration data using PSEQUAD computer program.[15]

$$pM + qL + rH \leftrightarrow M_pL_qH_r \quad (2)$$

$$\beta_{M_pH_qL_r} = \frac{[M_pH_qL_r]}{[M]^p[H]^q[L]^r} \quad (3)$$

The constants were calculated as the average of eight independent titrations. The applied ratios of the ligands and metal ions were 4:1, 2:1, and 1:1 with 4.97×10^{-3} M ligand concentrations. The concentration of metal stock solutions ($Ni(ClO_4)_2$) was determined by atomic absorption spectroscopy. No precipitation of the tetranuclear complex was observed during the titration even at strongly alkaline pH. This phenomenon is probably due to the very slow addition of base by autoburet since after a few hours the tetranuclear complex was slowly precipitated.

^1H NMR Spectroscopic Titration of Ligand αMeAla-Ha. The protonation constants of ligand αMeAla-Ha were also determined by pH-dependent ^1H NMR spectroscopic measurements. Sample of αMeAla-Ha (0.02 M) was prepared in H_2O, and the pH was adjusted with HCl and NaOH solutions. The pH was measured on an Orion 710A precision digital pH-meter using an Orion Ross Semimicro combined pH glass electrode, which was previously calibrated on three points with standard aqueous buffers (Prolabo). All measurements were performed at 298 K.

(9) Wienken, M.; Lippert, B.; Zangrando, E.; Randaccio, L. *Inorg. Chem.* **1992**, *31*, 1983.

(10) Alves, W. A.; Bagatin, I. A.; Da Costa Ferreira, A. M. *Inorg. Chim. Acta* **2001**, *321*, 11. Alves, W. A.; Cerchiaro, G.; Paduan-Filho, A.; Tomazela, D. M.; Eberlin, M. N.; Da Costa Ferreira, A. M. *Inorg. Chim. Acta* **2005**, *358*, 3581. Brown, S. J.; Olmstead, M. M.; Mascharak, P. K. *Inorg. Chem.* **1989**, *28*, 3720. Kolks, G.; Lippard, S. J.; Waszczak, J. V.; Lilienthal, H. R. *J. Am. Chem. Soc.* **1982**, *104*, 717. Koyama, N.; Watanabe, R.; Ishida, T.; Nogami, T.; Kogane, T. *Polyhedron* **2009**, *28*, 2001. Matsumoto, N.; Motoda, Y.; Matsuo, T.; Nakashima, T.; Re, N.; Dahan, F.; Tuchagues, J.-P. *Inorg. Chem.* **1999**, *38*, 1165. Shimazaki, Y.; Takani, M.; Yamauchi, O. *Dalton Trans.* **2009**, 7854. Sunatsuki, Y.; Motoda, Y.; Matsumoto, N. *Coord. Chem. Rev.* **2002**, *226*, 199. Higa, T.; Moriya, M.; Shimazaki, Y.; Yajima, T.; Tani, F.; Karasawa, S.; Nakano, M.; Naruta, Y.; Yamauchi, O. *Inorg. Chim. Acta* **2007**, *360*, 3304.

(11) Mukherjee, S.; Weyhermüller, T.; Bill, E.; Chaudhuri, P. *Eur. J. Inorg. Chem.* **2004**, 4209.

(12) Henry, B.; Gajda, T.; Selve, C.; Delpuech, J.-J.; Arnould, J. M. *Amino Acids* **1993**, *5*, 113.

(13) Rosotti, F. J. C.; Rosotti, H. *The determination of stability constants*; McGraw-Hill Book Co.: New York, 1961; p 149.

(14) Högfeldt, E. *Stability constants of metal-ion complexes, Part A*; Pergamon: New York, 1982; p 32.

(15) Zékány, L.; Nagypál, L. PSEQUAD. In *Computational Methods for the Determination of Stability Constants*; Legget, D., Ed.; Plenum: New York, 1985.

X-ray Crystallographic Study. CCDC 732319. Data of X-ray diffraction were collected at 100 K with Mo Kα radiation (λ = 0.71073 Å) on an Oxford Diffraction Atlas CCD diffractometer. The structure was solved by direct methods using SHELXS-97[16] program and refined with full-matrix least-squares on F^2 using SHELXL-97 program.[16] All the non-hydrogen atoms were refined with anisotropic temperature factors. Crystal data, data collection parameters, and results of the analyses are listed in Table 2. Supplementary crystallographic data for this structure (atomic coordinates, thermal parameters, and intramolecular bond distances and angles) are located in the Supporting Information (CIF file format).

Computational Details. All calculations were performed in the gas phase, with the Gaussian03 program package[17] (revision B.05) using density functional theory (DFT) with the hybrid exchange-correlation B3LYP functional.[18] The molecular structures were optimized using the 6-311G(d,p) basis set in the closed shell singlet state using default convergence criteria. The wave function stability was checked on the optimized structures, and frequency calculations were performed at the same level of theory in order to check that the optimized molecular structures correspond to true energy minima. Gaussian03 input files for the C_1 and S_4 symmetric tetramer (containing the optimized atomic coordinates) are given in Supporting Information. NMR chemical shifts were calculated on the optimized geometry S_4 using the GIAO method and the 6-311+G-(2d,p) basis set. Only one conformation was used for the NMR spectra calculation of the free ligand; the latter was obtained by optimization (B3LYP 6-311G(d,p)) of the protonated form of the ligand, in a conformation close to the one adopted in the complex. Calculated NMR data given in Table 4 and Supporting Information Table S1 are referred to TMS (calculated at the same level of theory) and also linearly scaled to the experimental data.[19]

Results and Discussion

Equilibrium Studies. Ligand Protonation. The potentiometrically determined macroscopic deprotonation constants of the imidazole group (K_1) and of the terminal amino group (K_2) in the free αMeAla-Ha ligand are listed in Table 1 as the formation constants β_{012} and β_{011}. The two deprotonation steps significantly overlap ($\Delta pK < 2$), suggesting the occurrence of alternative microdeprotonations. These microscopic deprotonation equilibria are shown in Scheme 1; the corresponding microscopic constants (k_a, k_i, k_a^i, k_i^a) can be determined by ^{1}H NMR spectroscopy from pH-dependent chemical shifts of nuclei in the vicinity of the proton binding site. The observed chemical shifts are given by eq 4

$$\delta_{obs} = x_{LH_2}\delta_{LH_2} + x_{LH}\delta_{LH} + x_L\delta_L \qquad (4)$$

where δ_{LH_2}, δ_{LH}, and δ_L are the chemical shifts of the protons in species LH_2, LH, and L, respectively, and x_{LH_2}, x_{LH}, and x_L are the molar fractions of these species. δ_{LH_2} and δ_L are obtained as the limit values of δ_{obs} on the extremities (acidic or basic) of the δ_{obs} vs pH titration curve. The first step in Scheme 1 corresponds to the deprotonation of either the amino group (k_a) or the imidazole ring (k_i) to yield the tautomeric forms LH_a and LH_i. Consequently, the chemical shift of LH should be given as a weighted mean of the two microspecies LH_a and LH_i (δ_{LH_a} and δ_{LH_i}, respectively). The concentration ratio of these two monoprotonated microspecies LH_a:LH_i is pH independent and equals to $k_a/k_i = k_i^a/k_a^i$.

The molar fractions can be expressed either by the equilibrium constants (left of eqs 5 and 6) or by the chemical shifts (right of eqs 5 and 6) leading to the final operational expressions for the fitting of experimental data (with index either a or i).

$$\frac{k_{a,i}[H^+] + K_1K_2}{[H^+]^2 + K_1[H^+] + K_1K_2} = \frac{\delta_{LH_2}^{a,i} - \delta_{obs}^{a,i}}{\delta_{LH_2}^{a,i} - \delta_L^{a,i}} \qquad (5)$$

$$\frac{K_1[H^+] + 2K_1K_2}{[H^+]^2 + K_1[H^+] + K_1K_2} = \sum_{a,i} \frac{\delta_{LH_2}^{a,i} - \delta_{obs}^{a,i}}{\delta_{LH_2}^{a,i} - \delta_L^{a,i}} \qquad (6)$$

The detailed calculation of macro- and microconstants from ^{1}H NMR measurements have been described earlier.[20]

Table 1. Formation Constants (log β) and Derived Data for the Proton and Nickel(II) Complexes of αMeAla-Ha

Species	*pqr*	log β_{pqr}[a]	p*K*
LH_2	012	14.88(1)	pK_1 = 6.75
LH	011	8.13(1)	pK_2 = 8.13
MLH	111	10.23(4)	pK_{MLH}^{ML} = 6.58
ML	110	3.65(4)	
MLH_{-1}	11−1	−3.20(1)	$pK_{ML}^{MLH_{-1}}$ = 6.85
ML_2	120	8.26(1)	
ML_2H_{-1}	12−1	0.63(1)	$pK_{ML_2}^{ML_2H_{-1}}$ = 7.63
$M_4L_4H_{-8}$	44−8	−35.10(2)	pK_{oligo}^{4} = 5.73

[a] The estimated errors are given in parentheses, I = 0.1 M $NaClO_4$, T = 298 K. $pK_{MLH}^{ML} = \log\beta_{110} - \log\beta_{111}$, $pK_{ML}^{MLH_{-1}} = \log\beta_{11-1} - \log\beta_{110}$, $pK_{ML_2}^{ML_2H_{-1}} = \log\beta_{12-1} - \log\beta_{120}$, $pK_{oligo}^{4} = \log\beta_{11-1} - {}^1/_4 \log\beta_{44-8}$.

Scheme 1. Schematic Representation of Macro- and Micro-Deprotonation Equilibria of αMeAla-Ha Ligand[a]

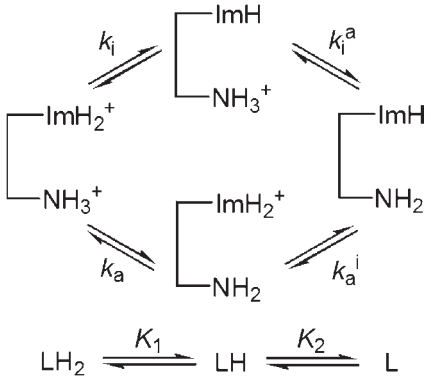

[a] LH_2 fully protonated ligand (charges omitted), LH (LH_a and LH_i) monoprotonated ligand, L neutral ligand. $K_1 = k_a + k_i$; $K_1K_2 = k_ak_a^i = k_ik_i^a$.[20]

(16) Sheldrick, G. M. *SHELXL-97 and SHELXS-97, Program for X-ray Crystal Structure Solution and Refinement*; University of Göttingen: 1997.

(17) Frisch, M. J.; Trucks, G. W.; Schlegel, H. B.; Scuseria, G. E.; Robb, M. A.; Cheeseman, J. R.; Montgomery, J. A.; Vreven, J., T.; Kudin, K. N.; Burant, J. C.; Millam, J. M.; Iyengar, S. S.; Tomasi, J.; Barone, V.; Mennucci, B.; Cossi, M.; Scalmani, G.; Rega, N.; Petersson, G. A.; Nakatsuji, H.; Hada, M.; Ehara, M.; Toyota, K.; Fukuda, R.; Hasegawa, J.; Ishida, M.; Nakajima, T.; Honda, Y.; Kitao, O.; Nakai, H.; Klene, M.; Li, X.; Knox, J. E.; Hratchian, H. P.; Cross, J. B.; Bakken, V.; Adamo, C.; Jaramillo, J.; Gomperts, R.; Stratmann, R. E.; Yazyev, O.; Austin, A. J.; Cammi, R.; Pomelli, C.; Ochterski, J. W.; Ayala, P. Y.; Morokuma, K.; Voth, G. A.; Salvador, P.; Dannenberg, J. J.; Zakrzewski, V. G.; Dapprich, S.; Daniels, A. D.; Strain, M. C.; Farkas, O.; Malick, D. K.; Rabuck, A. D.; Raghavachari, K.; Foresman, J. B.; Ortiz, J. V.; Cui, Q.; Baboul, A. G.; Clifford, S.; Cioslowski, J.; Stefanov, B. B.; Liu, G.; Liashenko, A.; Piskorz, P.; Komaromi, I.; Martin, R. L.; Fox, D. J.; Keith, T.; Al-Laham, M. A.; Peng, C. Y.; Nanayakkara, A.; Challacombe, M.; Gill, P. M. W.; Johnson, B.; Chen, W.; Wong, M. W.; Gonzalez, C.; Pople, J. A. *Gaussian 03*, Revision B.05, Gaussian, Inc.: Wallingford, CT, 2004.

(18) Becke, A. D. *J. Chem. Phys.* **1993**, *98*, 5648.

(19) Baldridge, K. K.; Siegel, J. S. *J. Phys. Chem. A* **1999**, *103*, 4038.

(20) Gajda, T.; Henry, B.; Delpuech, J. J. *J. Chem. Soc., Perkin Trans. 2* **1994**, 157.

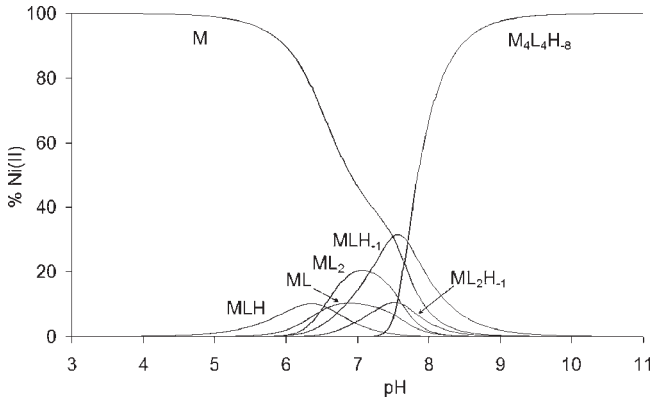

Figure 1. Concentration distribution of complexes in the Ni(II)-αMe-Ala-Ha system as a function of pH. [Ni(II)] = 4.97×10^{-3} M, [M]:[L] = 1:1.

In this work, the pH-sensitive chemical shifts of the imidazole (C8)H and (C9)H protons (type i) and of the N-terminal $(C2)H_3-(C3)H_3$ protons (type a) were used to calculate the macro- and microconstants (Supporting Information Figure S1). The macroconstants K_1 and K_2 were adjusted in the first step by fitting ^{1}H NMR data according to eq 6 leading to $pK_1 = 6.68 \pm 0.02$ and $pK_2 = 8.05 \pm 0.02$. These p*K*s slightly differ from the corresponding values obtained from the pH-metric technique, probably due to the imprecision of pH-electrode calibration on three points. The microconstants k_i and k_a were obtained as above in the second step using eq 5 (with index either a or i, separately) with the K_1 and K_2 values determined in the first step. The four microconstants are as follows: $pk_a = 7.68$, $pk_i = 6.73$, $pk_a^i = 7.06$, and $pk_i^a = 8.01$. The pH independent concentration ratio of LH_a:LH_i ($= k_a/k_i = k_i^a/k_a^i$) is 0.113, which corresponds to the relative amount of the minor tautomer (LH_a) of 10.15%. This result is interesting concerning the metal ion binding site in the MLH complex: either the imidazole or the amine nitrogen atom can bind the metal ion (vide infra).

Nickel(II) Coordination. Equilibrium study on the Ni-(II)-αMeAla-Ha system has been investigated between pH 3 and pH 11 by potentiometric titration combined with spectrophotometric experiments (vide infra). The formation constants are reported in Table 1, and the concentration distribution curves of species as a function of pH are shown in Figure 1 for [M]:[L] = 1:1 and in Supporting Information Figure S2 for [M]:[L] = 1:2.

The parent complex MLH formation started at pH ∼ 4.5. As shown above, in the free ligand the deprotonations of the amino and the imidazole groups overlap; consequently, the first metal-promoted deprotonation can also occur at either nitrogen atom. The proton release of the MLH complex leads to ML species involving two coordinated nitrogen atoms of terminal amino and imidazole groups. The determined formation constants β_{111} and β_{110} are close to the values found for Ni(II)-GlyHa (glycyl-histamine) and for Ni(II)-SarHa (sarcosyl-histamine).[6] Between pH 6 and pH 7.5 the predominant species is MLH_{-1}. This complex involves a N_3O coordination of N^3-imidazole, amino, and amide nitrogens with one molecule of water to complete the equatorial coordination sphere of nickel(II) ion. The value of the deprotonation constant $pK_{ML}^{MLH_{-1}} = \log \beta_{110} - \log \beta_{11-1} = 6.58$ is in good agreement with the values of 6.89 and 6.03 found for Ni(II)-GlyHa and Ni(II)-SarHa, respectively.[6] In the pH range 6.2−9, the bis-complexes ML_2 and ML_2H_{-1} are also formed. The close values of $pK_{ML_2}^{ML_2H_{-1}} = \log \beta_{11-1} - \log \beta_{110} = 7.63$ compared to Ni(II)-GlyHa (7.89) and Ni(II)-SarHa (7.94) suggests a similar deprotonation step as proposed earlier.[4−6] The species ML_2 can be denoted as MLH_{-1}(LH), where the water molecule in equatorial position of MLH_{-1} is replaced by another monodeprotonated ligand (N-amino or N-imidazole coordinated according to quantities of LH_a or LH_i, respectively). The species ML_2H_{-1} (= MLH_{-1}(L)) is derived from the deprotonation of this monodentate ligand.

Above pH = 7.5, a further deprotonation process can be detected and assigned to the proton loss of imidazole N^1 atom of MLH_{-1}. The species MLH_{-2} was not detected; it can readily oligomerize to form the imidazolate-bridged tetranuclear $M_4L_4H_{-8}$ species. The earlier published values of $pK_{oligo}^4 = \log \beta_{11-1} - {}^1/_4 \log \beta_{44-8}$ for nickel(II) tetranuclear complexes (7.32, α-hydroxymethylseryl-histidine (HmsHis);[7] 6.73, GlyHa; 6.58, SarHa[6]) are significantly higher than the constant reported in this work (5.73). This higher stability observed for αMeAla-Ha can be resulted from the more hydrophobic character of the two methyl groups.

UV−Visible Spectroscopy. Additional information on the species formation was obtained from UV−vis spectroscopic measurement as a function of pH in the range from 3 to 11.

The UV−vis spectra did not show modification with pH change to ∼6. The three bands observed at 725, 660, and 394 nm can be attributed to octahedral nickel(II) complex (Supporting Information Figure S3). The MLH and ML complexes are only minor species (in ∼10% quantities, Figure 1) and exhibit only weak absorption;[8] thus, they could not be spectroscopically identified. Above pH = 6, the color of the solution changed from light green to yellow (λ_{max} = 440 nm, Supporting Information Figures S3 and S4), indicating the formation of new diamagnetic complex-(es) with square planar arrangement around the nickel(II) ion. Morris et al. have reported the spectral changes for Ni(II)-glycyl-L-histidine.[8] They concluded that the development of a yellow diamagnetic Ni(II)-complex should not occur on simple replacement of H_2O by OH^- in the metal coordination sphere, and the spectral changes must involve the replacement of water in the fourth equatorial coordination position by a nitrogen donor atom. In the case of αMeAla-Ha ligand, an N_4 equatorial binding site was proposed for the species ML_2 and ML_2H_{-1}, where the complex formation starts at pH 6. For the reported Ni(II)-dipeptide containing systems (GlyHa, SarHa) the bis-complexes (ML_2 and ML_2H_{-1}) are present in very low quantities (< 10% if [M]:[L] = 1:1) preventing the detection by UV−vis spectroscopy. These results suggest that the bis-complexes formed with αMeAla-Ha ligand are diamagnetic and the nickel(II) ion has a square planar geometry.

At higher pH (> 7) the d−d transition observed at 440 nm was not shifted, only the intensity of this band increased significantly up to pH 8.5 indicating the formation of oligomeric species (ε = 520 $L \cdot mol^{-1} \cdot cm^{-1}$, Supporting Information, Figure S4).

Synthesis and Structure of [Ni(αMeAla-Ha)]$_4$ (1). The cyclic tetramer **1** was prepared by mixing equimolar aqueous solution of αMeAla-Ha and $Ni(ClO_4)_2$. During

the pH adjustment to 10 by 0.1 M NaOH solution, a yellow precipitate formed immediately. After filtration and recrystallization from MeOH, yellow prisms suitable for X-ray structure determination were obtained. The crystallographic data for **1** are collected in Table 2, and selected bond distances are given in Table 3. In the structure of **1** (Figure 2 left), the four Ni(αMeAla-Ha) units are connected by a coordination bond between the nickel(II) ion and the imidazole N^1 atom of the adjacent ligand, forming a cyclic assembly (N4, N8, N12, and N16 on Figure 2). The square planar coordination sphere around each nickel was further completed by the amino nitrogen, the deprotonated amide nitrogen, and imidazole N^3 atom of the ligand (N3, N7, N11, and N15 on Figure 2). The four N donors are coplanar within 0.09 Å, and the metal ion is up to the least-squares plane of the four coordinated nitrogens within 0.04 Å. The N−Ni−N angles depend on the size of the chelate ring: the N_{amine}−Ni−N_{amide} angle is smaller (between 83.5° and 85.1°) than N_{amide}−Ni−N_{im} (between 93.4° and 93.9°) due to the more rigid five-membered ring. Most structural parameters (distances and angles) are close to the values determined for the Ni(II)-glycyl-glycyl-α-hydroxy-D,L-histamine[21] and Ni(II)-triglycyl-glycine[22] complexes. In nonpeptidic environment, the sole tetranuclear structure with imidazolate bridged nickel(II) ions was determined with a Schiff-base ligand containing a phenolate and an imidazolate group.[11] Each nickel(II) ion is in a distorted

Table 2. Crystal Data and X-ray Experimental Parameters for [Ni(αMeAla-Ha)]$_4$ (**1**)

	1·4.5CH_3OH·1.5H_2O
formula	$C_{36}H_{56}N_{16}Ni_4O_4$·4.5$CH_3OH$·1.5$H_2O$
formula weight	1182.92
crystal system	monoclinic
space group	$P2_1/c$ (No. 14)
a, Å	11.2645(4)
b, Å	23.5003(8)
c, Å	20.9007(7)
α, deg	90
β, deg	102.321(1)
γ, deg	90
V, Å^3	5405.4(3)
Z	4
D_{calcd}, g·cm^{-3}	1.423
T, K	100(2)
μ(Mo Kα), cm^{-1}	1.435
no. of reflns measd	23958
no. of indep reflns	12358
no. of obsd reflns	8441 ($I > 2\sigma(I)$)
R ($F^2 > 2\sigma(F^2)$)	0.0576[a]
R_w (F^2)	0.1737[a]
GOF	0.931

[a] $w = 1/[\sigma^2(F_o^2) + (0.0918P)^2 + 18.8285P]$ where $P = (F_o^2 + 2F_c^2)/3$.

Table 3. Selected Bond Distances (Å) for [Ni(αMeAla-Ha)]$_4$ (**1**) from X-ray Data and from Theoretical Calculation (*data in italics*)

	Measured	*Calculated*			Measured	*Calculated*	
		C1 symmetry	*S4 symmetry*			*C1 symmetry*	*S4 symmetry*
Ni1−N1	1.911(5)	*1.930*	*1.931*	Ni3−N16	1.888(4)	*1.917*	
Ni1−N2	1.860(5)	*1.881*	*1.881*	Ni4−N13	1.905(5)	*1.933*	
Ni1−N3	1.884(4)	*1.895*	*1.888*	Ni4−N14	1.889(4)	*1.885*	
Ni1−N8	1.881(5)	*1.915*	*1.914*	Ni4−N15	1.888(5)	*1.897*	
Ni2−N5	1.900(5)	*1.929*		Ni4−N4	1.895(4)	*1.917*	
Ni2−N6	1.883(5)	*1.875*		Ni1···Ni2	5.774	*5.789*	*5.845*
Ni2−N7	1.879(5)	*1.895*		Ni2···Ni3	5.752	*5.850*	
Ni2−N12	1.892(5)	*1.920*		Ni3···Ni4	5.774	*5.892*	
Ni3−N9	1.907(4)	*1.930*		Ni4···Ni1	5.832	*5.866*	
Ni3−N10	1.882(5)	*1.878*		Ni1···Ni3	6.111	*6.876*	*7.586*
Ni3−N11	1.898(4)	*1.894*		Ni2···Ni4	6.782	*7.256*	

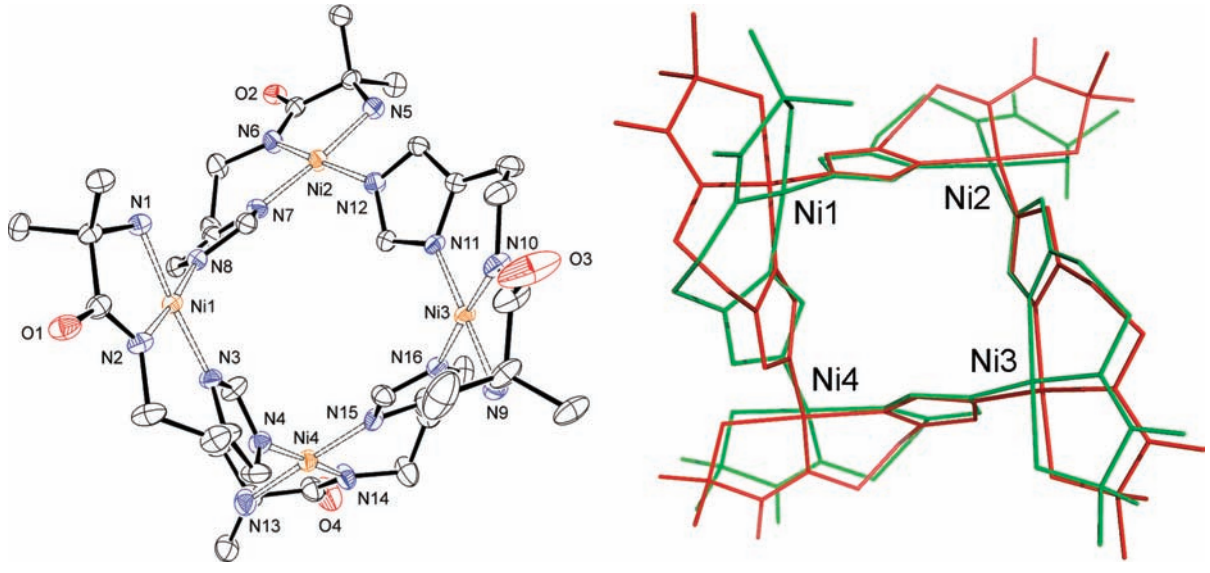

Figure 2. Left: ORTEP drawing of the neutral [Ni(αMeAla-Ha)]$_4$ (**1**) complex showing 50% probability ellipsoids. Hydrogen atoms and solvent molecules are omitted for clarity. Right: DFT optimized molecular structures of complex **1** in C_1 (green) and S_4 (red) symmetries (the structures were superposed through the four Ni atom pairs). These molecular structures differ from the CH_2−CH_2 torsion angle of the ligand bridging Ni1 to Ni4.

square-planar geometry with N_3O coordination from phenolate oxygen, imine nitrogen, imidazole N^3, and adjacent imidazole N^1 atoms. The measured distances and angles for Ni−N^3 and Ni−N^1 are close to the values reported in this work.

On the basis of the tetrameric structure of gold(III) glycyl-L-histidine[9] and space-filling molecular models,[8] a C_2 symmetrical structure was proposed for the $M_4L_4H_{-8}$ tetramer in the literature.[5,7] It suggests that the imidazole ring is approximately parallel to the coordination plane of the metal center in the same unit and roughly perpendicular relatively to the coordination plane of the adjacent unit, as well as that the two imidazole rings are in cis position around the metal ion. The linkage of two superimposable dimers formed in this manner gives the cyclic structure with a C_2 symmetrical saddle-like shape.

An interesting aspect of structure **1** is the position of the imidazole rings. In the same unit, the imidazole rings are tilted from the parallel plane (from 10.1° to 28.5°). Between two units, the angles of 4N−metal coordination plane-adjacent imidazole plane are close to perpendicular (78.4°, 86.3°, and 73.3°) except for one where this angle is 41.9°. Consequently, **1** does not possess any symmetry axis in the solid state, all atoms being unique in the tetramer. However, DFT calculations performed in the gas phase indicate that S_4 symmetric tetramer, where the four units are equivalent, is more stable by 11 kJ·mol^{-1} than the non symmetric C_1 structure. The superposition of the S_4 and C_1 symmetric optimized molecular structures (Figure 2 right) clearly shows that the main difference between the two structures is the inversion of the CH_2−CH_2 torsion angle of the ligand associated with Ni1. Compared to the case of gold(III) glycyl-L-histidine, **1** can adopt a more symmetric structure due to the lack of asymmetric carbon in the α-methyl-alanyl-histamine ligand.

The solvent model contains only MeOH and water molecules. The best model found is given in the Cif file and shown in the Supporting Information Figures S5 and S6, where a mixture of MeOH and H_2O gives disordered fragments with 0.5 occupancies. Eleven hydrogen atoms of solvent molecules were not localized due to the disorder. Residual peaks of electron density are 1.99 e·Å^{-3} at 0.0688 0.3954 0.1135 (0.86 Å from Ni4), and the second one of 1.2 e·Å^{-3} in the disordered solvent molecules (C40B−O40B, C41B−O41B, OW2A). This peak can not be attributed to these molecules as the H atom.

The complex **1** has the possibility to accommodate small guests due to its saddle-like shape with quite long metal−metal distances (6.111 and 6.782 Å). Despite this fact no molecule "trapped" inside the tetramer was found.

NMR Spectroscopy. The diamagnetic character of Ni(II) ion in square planar geometry allows the structural study of complex **1** in solution by NMR spectroscopy. The imidazole region of the ^{1}H NMR spectrum of **1** presents only two signals at 6.81 ppm and 5.39 ppm corresponding to (C8)H and (C9)H, respectively (or C^5−H and C^2−H using the IUPAC convention, Figure 3 and Supporting Information Figure S7). A slight shift was observed for (C8)H compared to the free ligand (6.85 ppm); however, (C9)H was considerably upfield shifted (free ligand 7.57 ppm). DFT GIAO NMR calculations performed on the free ligand and on the optimized **1** (S_4 symmetry) reproduce these shifts, although with a slight differing amplitude (for (C9)H: from 7.55 in free ligand to 5.83 ppm in **1**; Table 4). Gajda et al., and later Gizzi et al., have observed less significant upfield shift for Xaa-Yaa-Histamine tripeptide at alkaline pH, where there was only N^1−H deprotonation and no pyrrole-like metal coordination (N^1−H corresponds to (N4)H in the case of complex **1**).[2] These facts suggest that, in our case, such an important shift is due to the involvement of both imidazole nitrogens in metal ion coordination. Furthermore, the ^{1}H and ^{13}C NMR equivalences of imidazole parts in **1** indicate that there is no difference in solution between the Ni(αMeAla-Ha) units (Table 4 and Supporting Information Table S1).

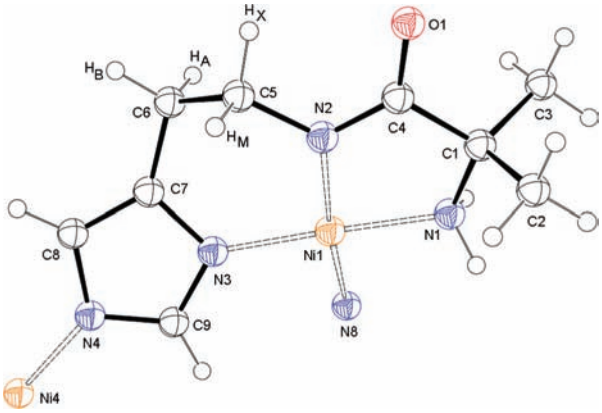

Figure 3. ORTEP drawing of one Ni(αMeAla-Ha) unit of complex **1** in solid state showing 50% probability ellipsoids.

Wienken et al. has recorded the ^{1}H NMR spectrum of structurally characterized gold(III) glycyl-L-histidine tetramer and observed two sets of imidazole C^2−H and C^5−H protons with identical intensities as the consequence of C_2-symmetry of the cyclic tetramer.[9] Mlynarz et al. has come to the same conclusion from the ^{1}H NMR study of the Ni(II)-α-hydroxymethylseryl-histidine system at pH above 10.[7] However, Gajda et al. has observed only one set of imidazole C^2−H and C^5−H protons and concluded the existence of cyclic tetramer with glycyl-histamine ligand.[6] In the case of complex **1**, the observed discordance between X-ray (inequivalence of the 4 units) and NMR (equivalence of the 4 units) measurements may be due to the fast molecular rearrangement in solution or to symmetry breaking upon crystallization of the S_4 symmetric structure.

The ^{1}H NMR spectrum of complex **1** exhibits inequivalences for the aliphatic part of histamine, which gives rise to an ABMX spin system (Figure 4, bottom). The resonance of the proton nuclei bound to C5 is upfield shifted relative to the free ligand (3.43 ppm) and separated in two multiplet signals H_M and H_X. The multiplet at 2.6 ppm corresponds to the part AB of the ABMX spin system and can be assigned to the protons bound to C6.

We performed a simulation of this region of the NMR spectrum (program ECHGN[23]) to obtain the values of the coupling constants (in Hz) $J_{AB} = -14.73$, $J_{AM} = 10.95$, $J_{AX} = 3.45$, $J_{BM} = 3.07$, $J_{BX} = 4.88$, and $J_{MX} = -13.00$ and

(21) Bal, W.; Djuran, M. I.; Margerum, D. W.; Gray, E. T. J.; Mazid, M. A.; Tom, R. T.; Nieboer, E.; Sadler, P. J. *J. Chem. Soc., Chem. Commun.* **1994**, 1889.

(22) Freeman, H. C.; Guss, J. M.; Sinclair, R. L. *Acta Crystallogr., Sect. B* **1978**, *34*, 2459.

(23) Delpuech, J.-J. ECHGN computational program, unpublished work.

Table 4. Experimental (in MeOH-d_4 at 298 K) and Calculated ^{1}H NMR Chemical Shifts (in ppm) of Ligand αMeAla-Ha and Complex **1**

	(C9)H	(C8)H	(C5)H_2	(C6)H_2	(C3)H_3, (C2)H_3	
			αMeAla-Ha			
experimental data	7.57	6.85	3.43	2.78	1.27	
calculated data[a]	7.55	6.78	3.59[b]	2.55[b]	1.25[b]	
calcd scaled to exptl data	7.57	6.81	3.63[b]	2.59[b]	1.30[b]	
			Complex **1**			
experimental data	5.39	6.81	2.22 (M) 3.09 (X)	2.58 (A) 2.61 (B)	1.41 1.27	
					(C2)H_3	(C3)H_3
calculated data[a]	5.83	6.99	1.99 (M) 3.92 (X)	2.53 (A) 2.51 (B)	1.51[b]	1.08[b]
calcd scaled to exptl data	5.47	6.52	1.99 (M) 3.74 (X)	2.46 (A) 2.48 (B)	1.55[b]	1.16[b]

[a] GIAO DFT B3LYP 6-311+G(2d,p), reference TMS. [b] Average value for the two CH_2 and for the three CH_3 protons.

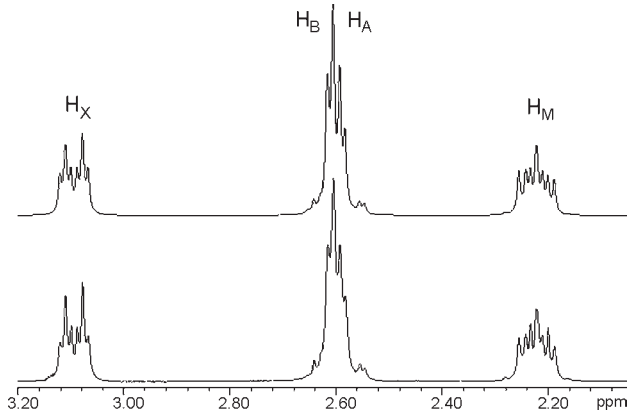

Figure 4. Simulated (top) and experimental (bottom) ^{1}H NMR spectrum of complex **1** in MeOH-d_4.

the chemical shifts (in ppm) $\delta_A = 2.585$, $\delta_B = 2.607$, $\delta_M = 2.217$, and $\delta_X = 3.088$ (Figure 4, top). By means of NMR NOESY experiment it was possible to assign protons H_M and H_X in the structure of the complex. Since the chemical shifts of H_A and H_B nuclei are very close to each other, the integrals of cross-peaks give information only on the proximity of these protons without distinction. It appears that H_M is the nucleus separated by the longer distance from H_A and H_B (Supporting Information Figure S8). DFT GIAO NMR calculations also found very close chemical shifts for H_A and H_B nuclei in **1**. The relative shifts of H_M and H_X protons attached to C5 in the complex are also well reproduced in the calculations (M upfield compared to X, Table 4).

The Karplus equation describes the correlation between $^3J_{H,H}$ coupling constants and dihedral torsion angles (θ) and thus allows NMR measurement in solution to be connected with X-ray analysis in solid state. The relationship $^3J_{H,H} = 5.1 \cos 2\theta - 1.8 \cos \theta + 7$ determined for peptidic environment was used to calculate θ_{calcd} dihedral angles.[24] The H_A−C6−C5−H_X and H_B−C6−C5−H_X dihedral angles associated to J_{AX} and J_{BX} coupling constants have the values of 60.8° and 50.5°, respectively. The more important difference in the coupling constant values was measured for the proton H_M relative to H_A and H_B, which corresponds to the dihedral angles H_A−C6−C5−H_M and H_B−C6−C5−H_M of 149.1° and 64.0°, respectively. On the basis of these calculations we can show that the proton H_A is more distant from H_M with the highest dihedral angle than from H_X. Consequently, the relative position of four protons can be

(24) Cung, M. T.; Marraud, M. *Biopolymers* **1982**, *21*, 953.

Table 5. Average Lengths (calculated for four units) of Selected Distances (Å) and Averages (calculated for four units) of the Absolute Values of Selected Dihedral Torsion Angles (deg) from the X-ray Structure of Complex **1**

distances		dihedral torsion angles	
H_A−H_X	2.363	H_A−C6−C5−H_X	63.1
H_B−H_X	2.316	H_B−C6−C5−H_X	54.6
H_A−H_M	2.849	H_A−C6−C5−H_M	178.8
H_B−H_M	2.364	H_B−C6−C5−H_M	63.4

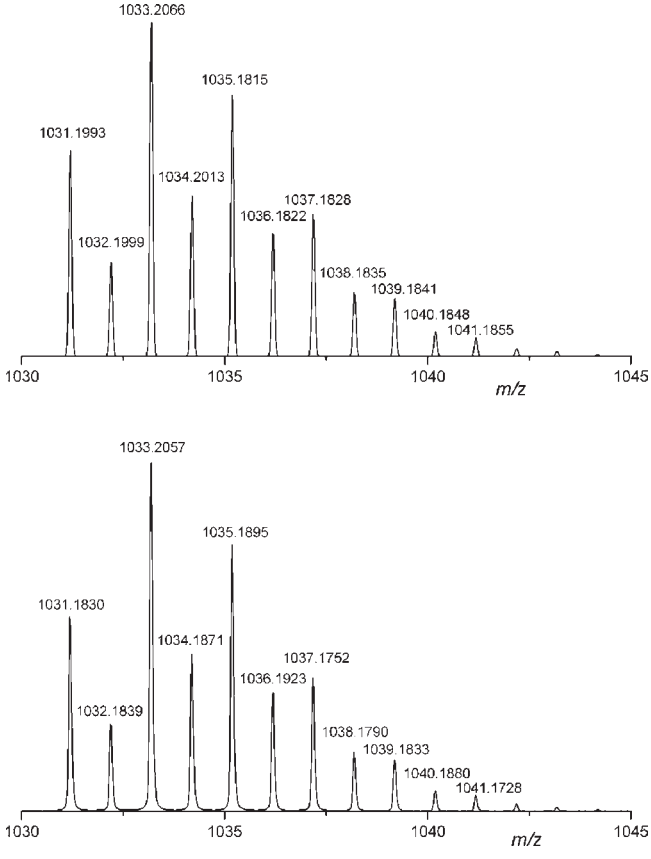

Figure 5. The molecular ion peak in the ESI-HR mass spectrum (positive) for complex $[C_{36}H_{56}N_{16}Ni_4O_4+Na]^+$ ($z = 1$) in MeOH with simulated (top) and observed (bottom) isotopic distribution.

unambiguously determined as shown in Figure 3. These results are in good agreement with those of the crystallographic analysis, except for the $H_A-C6-C5-H_M$ dihedral angle, where the experimental value is 178.8° in the X-ray structure (Figure 3, Table 5). This difference may be due to the empirical nature of the constants in the Karplus equation.

Mass Spectroscopy. The tetrameric structure in solution (MeOH) was also confirmed by ESI-HR mass spectroscopy. Two major signals are observed at m/z 1033 ($z = 1$) and 528 ($z = 2$) corresponding to the adduct of complex **1** with sodium ion $[C_{36}H_{56}N_{16}Ni_4O_4+Na]^+$. Two additional signals are present at m/z 1011 ($z = 1$) and 517 ($z = 2$) attributed to the tetranuclear $[C_{36}H_{56}N_{16}Ni_4O_4+H]^+$ complex ion (Supporting Information Figure S9). The isotopic pattern is in excellent agreement with the theoretical one without loss of mass resolution (Figure 5). This result, to the best of our knowledge, has never been published before for such a Ni(II)-containing tetranuclear compound.

Conclusion

The present work provides new information about the self-assembly process of metal-peptide clusters induced by metal$-N^1$-imidazole coordination in basic conditions. The crystal structure of tetranuclear $M_4L_4H_{-8}$ compound, which has been evoked several times in the literature, was determined for the first time with nickel(II) ion and a pseudodipeptide. The solid state structure possesses four nonequivalent units giving a C_1 symmetrical assembly. In solution, the formation of monomeric (MLH, ML, MLH_{-1}), bis (ML_2, ML_2H_{-1}), and tetrameric ($M_4L_4H_{-8}$) species was observed. The diamagnetic square planar geometry was proposed for the bis-complexes. Unfortunately, the presence of octahedral and thus paramagnetic species (MLH, ML, MLH_{-1}) does not allow the structural characterization of these bis-complexes by NMR spectroscopy. The hydrophobic character of the methyl groups in the αMeAla-Ha ligand promotes the tetrameric $M_4L_4H_{-8}$ species formation. This result emphasizes the fact that small structural changes in the ligand framework can influence sensitively the self-assembly process. The nuclearity was also confirmed in solution by ESI-HRMS analysis. NMR analysis in solution suggests a tetranuclear structure of symmetry S_4. On the basis of the results of DFT calculations, the structural differences observed in solution and in solid state were explained.

Acknowledgment. The Institut Jean Barriol (Nancy Université) and GENCI-CINES (Grant 2009-X2009-085106) are thanked for providing access to computational facilities. E. Wenger for the crystal structure determination, J.-J. Delpuech for the simulation of NMR spectrum by the program ECHGN, and S. Parant for technical help are kindly acknowledged. The authors thank B. Fernette for assistance in NMR measurements and F. Dupire for MS measuring.

Note Added after ASAP Publication. This paper was published on the Web on August 19, 2010, with an error in Scheme 1. The corrected version was reposted on August 25, 2010.

Supporting Information Available: CIF file giving crystallographic data for **1**, structural, potentiometric, NMR, and UV−visible spectroscopic data; and Gaussian03 input files. This material is available free of charge via the Internet at http://pubs.acs.org. Crystallographic data also available from The Cambridge Crystallographic Data Centre via www.ccdc.cam.ac.uk/data_request/cif.